Preprints of the 21st IFAC World Congress (Virtual)
Berlin, Germany, July 12-17, 2020

A Modified SDRE-based Sub-optimal Hypersurface Design in SMC ⋆

Sinan Ozcan * **Engin H. Copur** ** **Ahmet C. Arican** *** **Metin U. Salamci** ****

* *Turkish Aerospace, Ankara, 06980 Turkey (e-mail: siozcan@tai.com.tr).*
** *Astronautical Engineering Department, Necmettin Erbakan University, Konya, 42140 Turkey (e-mail: ehcopur@erbakan.edu.tr)*
*** *Mechanical Engineering Department, Gazi University, Ankara, 06570 Turkey, (e-mail: ahmetcagriarican@gazi.edu.tr)*
**** *Mechanical Engineering Department, Gazi University, Ankara, 06570 Turkey, (e-mail: msalamci@gazi.edu.tr)*

Abstract: Sliding Mode Control (SMC) plays a prominent role in dealing with matched uncertainties. In classical SMC design, the sliding surface (SS) is crucial to the guarantee for the stability and desired performance, especially if the system is nonlinear. A possible way to fulfill these desired performances for nonlinear systems is to use State Dependent Riccati Equation (SDRE) method, enabling SS to be designed even optimally. However, SDRE may suffer an inherent stability problem as well as a computational burden. To overcome these issues, in a recent study, a new SDRE method has been proposed. Therefore, this study takes advantages of the advanced SDRE method in designing a sub-optimal SS and also provides some comparative results with the conventional one to establish the feasibility of the proposed SDRE-based SMC control architecture experimentally. Experiments are conducted by using a 3-DOF helicopter platform and the results reveal that the proposed SDRE-based SMC is able to produce smoother SS than the conventional counterpart.

Keywords: Sliding-mode control, sliding surfaces, optimal control, nonlinear control systems, robust control.

1. INTRODUCTION

Sliding mode control (SMC) is one of the most effective robust control methods to offer a strong invariance property against matched uncertainties for complex high-order nonlinear systems (Utkin, 1977; Yu and Kaynak, 2016). Owing to its invaluable essence, SMC is capable of providing a highly successful control performance even when there only exists a modest model of a real system in the absence of high frequency dynamics (Lee and Utkin, 2007; Yu and Kaynak, 2016) and thereby enables an easy design process. In a conventional SMC, system's state trajectories move typically through two phases. In the reaching phase, system states are directed to a predefined sliding surface (SS) while in the sliding phase, they are forced to remain on this surface (Tai and Lu, 2006). This two-stage motion owes its existence to a design process consisting of two parts: (i) a SS, i.e. a kind of hypersurface, is obtained such that the controlled system possesses the desired dynamic characteristics and (ii) the design of a variable structure control law (Yan et al., 2017).

In literature, a large amount of research on linear SS design have been conducted for linear systems subject to uncertainties since 1960s (Edwards et al., 2018). However, a linear SS for a nonlinear system may not always guarantee either the stability or the desired performance criteria (Salamci and Gökbilen, 2007). Therefore, researchers have directed their attention to designing nonlinear SS. Some nonlinear hypersurfaces have been previously used for a finite-time convergence and elimination of reaching phase (Mobayen et al., 2017; Adhikary and Mahanta, 2018; Corradini and Cristofaro, 2018) as well as improving the transient response characteristics (Mobayen and Baleanu, 2015). In optimal control applications, a SMC with nonlinear SS is also capable of decreasing the amount of energy consumed by an industrial machine in operation. In accordance with this aim, Farrage and Uchiyama (2018) have developed a contouring controller including contouring error in nonlinear SS for a biaxial feed drive system. Another optimal problem of SMC is to design a SS enabling system states to consume minimal energy during sliding phase by minimizing a quadratic cost function (Pieper and Surgenor, 1993).

Amongst other optimal methods, State-Dependent Riccati Equation (SDRE) has attracted a great attention due to its ability to provide a flexible and systematic way to design a sub-optimal controller for a class of nonlinear systems (Çimen, 2012). Accordingly, SDRE has been greatly exploited in SS design. In the missile autopilot design, a SDRE-based SMC was developed by Salamci and Gökbilen (2007). Then Bilgin and Salamci (2014)

⋆ This study was supported under DKTM/2015/07 project by Turkish Aerospace.

have integrated it with approximating sequence method to eliminate the reaching phase. For a re-entry vehicle control with the parameter uncertainties and disturbances, an adaptive SMC was designed by using a SDRE-based optimal sliding surface (Liang et al., 2013). In a recent study (Ozcan et al., 2019), another SDRE-based SMC was proposed to eliminate the reaching phase in the design of the nonlinear SS for a nonlinear MIMO dynamical system and its global stability has been proven by Lyapunov theory. This method has also provided successful experimental results in the control of a helicopter within a wide range flight envelope.

Despite the fact that SDRE method gains a great advantage through the selection of weighting matrices and state-dependent coefficient (SDC) matrices, it may suffer from either a possible instability or excessive computational load because of its classical implementation. In a recent study conducted by Copur et al. (2019), these issues have been addressed in detail and a new SDRE method has been proposed to avoid these issues without a degradation in control performance. In the novel SDRE method, an Algebraic Riccati Equation needs to be solved in the re-computation of SS only when system states of interest are enough close to the boundary of a ball-shaped stability region. Additionally, this closeness can be easily determined by checking a Lyapunov's indirect method based condition.

In this study, the novel SDRE method is integrated with the design process of an optimal SS for SDRE-based SMC to guarantee the existence of a stable nonlinear SS as well as to reduce the computational load, thereby enhancing its implementability. To design the optimal nonlinear SS, a finite-time continuous SDRE is solved at each instant of time by minimizing a quadratic cost function consisting of weighting matrices, system states and control inputs. Çimen (2010) has previously stated that the selection of weighting matrices has great effect on control performance. Therefore, to improve the control performance of the proposed SDRE-based SMC, state-dependent weighting matrices are used while solving the finite-time continuous SDRE. To examine the effectiveness of the proposed SDRE-based SMC in a tracking control application in real-time, a 3-DOF laboratory helicopter is utilized to carry out the experiments. This test setup is a well-known platform for assessing the performance of the state-of-the-art control methods.

The paper is organized as follows: Section 2 explains the traditional method to design SDRE-based SMC. Section 3 presents the design procedure of an optimal sliding surface based on the new SDRE method. Section 4 presents a brief description of 3-DOF helicopter model and the design process of the proposed controller based on the model. Section presents the experimental results. Finally, Section gives the conclusion.

2. SDRE-BASED SMC METHOD

Consider the nonlinear system given by

$$\dot{x} = A(x)\,x + B(x)\,u,\ x(0) = x_0 \tag{1}$$

where $A(x) : \mathbb{R}^n \to \mathbb{R}^{n\times n}$ and $B(x) : \mathbb{R}^n \to \mathbb{R}^{n\times m}$ are known as State Dependent Coefficient (SDC) matrices with the state vector $x \in \mathbb{R}^n$ used to generate a state-feedback control law $u \in \mathbb{R}^m$. In SMC design, the nonlinear system (1) consisting of matrix and vector-valued functions is restructured such that

$$\dot{\tilde{z}} = A_{11}(z)\tilde{z} + A_{12}(z)\hat{z} \tag{2}$$

$$\dot{\hat{z}} = A_{21}(z)\tilde{z} + A_{22}(z)\hat{z} + B_2(z)u, \tag{3}$$

by a transformation matrix $T(x)$, resulting from $z = T(x)x$ where $z = [\tilde{z}\ \hat{z}]^\top$ with $\tilde{z} \in \mathbb{R}^{n-m}$ and $\hat{z} \in \mathbb{R}^m$. Since $T^{-1}(x)$, $\forall x \in \mathbb{R}^n$ is always non-singular, $B(x)$ can be reduced to a non-singular matrix of $B_2(z) \in \mathbb{R}^{m\times m}$, $\forall z \in \mathbb{R}^n$. This reorganization of the nonlinear system (1) enables a quasi-linear manifold, or referred to as SS, in terms of the new coordinates z to be defined as

$$\sigma(\tilde{z}, \hat{z}) = \hat{z} + C(z)\tilde{z}. \tag{4}$$

where $C(z)$ is the slope of SS. By virtue of the fact that $\sigma(\tilde{z}, \hat{z}) = 0$ during the sliding phase, $\hat{z} = -C(z)\tilde{z}$, and thereby the null space dynamics in (2) takes the form of

$$\dot{\tilde{z}} = [A_{11}(z) - A_{12}(z)C(z)]\,\tilde{z} = A_{cl}(z)\tilde{z}. \tag{5}$$

Now, $C(z)$ can be computed by using SDRE method in such a quasi-optimal way that $A_{cl}(z)$ becomes a pointwise Hurwitz matrix, i.e., $\mathrm{Re}\left[\lambda_{i=1,\dots,n}\left(A_{cl}\left(z\right)\right)\right] < 0$, $\forall z$ if the following lemma is satisfied.

Lemma 1. If $(A(x), B(x))$ pair in (1) is controllable for all x, then $(A_{11}(z), A_{12}(z))$ pair in (2) is also controllable for all z.

Proof. See Utkin (1992).

Thus, SDRE method provides a state-dependent nonlinear slope for the SS in (4) as follows:

$$C(z) = R^{-1}(z)A_{12}^\top(z)P(z)\tilde{z} \tag{6}$$

where $P(z)$ is the solution of finite-time SDRE, given by

$$\begin{aligned} A_{11}^\top(z)P(z) + P(z)A_{11}(z) - P(z)A_{12}(z) \\ \cdot R^{-1}(z)A_{12}^\top(z)P(z) + Q(z) = -\dot{P}(z) \end{aligned} \tag{7}$$

to minimize a quadratic cost function

$$J = \frac{1}{2}\int_0^\infty \left\{\tilde{z}^\top(t)\,Q\left(z\right)\tilde{z}\left(t\right) + \hat{z}^\top(t)\,R\left(z\right)\hat{z}\left(t\right)\right\} dt$$

subject to (2). Here, $Q(z)$ and $R(z)$ are semi-positive definite and positive definite weighting matrices, respectively. Unfortunately, there does not exist any method to obtain a global SDC parametrization for the nonlinear system (1) and select the weighting matrices for a optimum SDRE solution (Çimen, 2012), hence leading to a quasi-optimal SS subjected to $\sigma(\tilde{z}, \hat{z})\dot{\sigma}(\tilde{z}, \hat{z}) < 0$.

Then, the control structure u in the range dynamics (3) can be synthesized by combining two control components. Accordingly, this special form of the variable structure control becomes

$$u = u_{ec} + u_{sc} \tag{8}$$

where u_{ec} and u_{sc} are, respectively, the equivalent control component and the switched control component. Having derived it from $\dot{z}_2 + C(z)\dot{z}_1 = 0$ when $\dot{\sigma}(\tilde{z}, \hat{z}) = 0$, the former can be defined as

$$\begin{aligned} u_{ec} = &- B_2^{-1}\{A_{21}(z)\tilde{z} + A_{22}(z)\hat{z} \\ &+ C(z)\left[A_{11}(z)\tilde{z} + A_{12}(z)\hat{z}\right] + \dot{C}(z)\tilde{z}\} \end{aligned} \tag{9}$$

while the latter is given by

$$u_{sc} = -B_2^{-1}k\mathrm{sgn}\left(\sigma(\tilde{z}, \hat{z})\right) \tag{10}$$

where $k > 0$ and higher k offers shorter reaching phase but in turn higher amplitude of chattering, i.e. high frequency signal. Since the switched control part produces chattering, the signum function may be replaced by tanh fuction in order to suppress the effect of high frequency chattering in the control signal. In addition, $\dot{C}$ in (9) can be approximated numerically by

$$\dot{C}(z) \approx \frac{s}{T_f s + 1} C(z)$$

where T_f is the time constant of the first-order filter.

3. MODIFIED SDRE-BASED SMC

The standard implementation of SDRE method is based on solving an Algebraic Riccati Equation (ARE), like (7), at each instant by using a sample-data form of a SDC model for a class of nonlinear systems. This need causes higher computational effort for more complex nonlinear systems. In addition, SDRE method guarantees the stability at each instant. Yet, in between these time steps, an instability may occur. These issues have been addressed in detail by Copur et al. (2019). Then, for solving them, Copur et al. (2019) have also adapted the standard SDRE method. This new approach does not require the solution of ARE whenever a Lyapunov's indirect method based condition is satisfied. Therefore, it can remarkably reduce the computational burden as well as readily avoid the instability between instants, as compared to the conventional. Now, before briefly introducing the modified SDRE approach to design the sub-optimal SS in (4), some definitions are given for the sake of clarity.

Definition 2. Let $z_i \in \mathbb{R}^{n-m}$, $(i = 0, \ldots, p)$ be some system states in (5) in succession, but not necessarily in consecutive order.

Definition 3. Let $V_i : \Omega_i \to \mathbb{R}$ be a Lyapunov function that satisfies the conditions of the asymptotic stability.

Definition 4. Let $\Omega := \bigcup_{i=1}^{p} \Omega_i$, that is to say formed by the glued stable regions Ω_i, and $\Omega = \{\tilde{z} \in \mathbb{R}^{n-m} : \|z_0\| < r\}$, which is a non-local stable region.

With Definition 2, the null space dynamics (2) can take intrinsically the linear form of

$$\dot{\tilde{z}} = A_i \tilde{z} + B_i \hat{z} \tag{11}$$

where $A_i = A_{11}(z)|_{z=z_i}$ and $B_i = A_{12}(z)|_{z=z_i}$.

Theorem 5. Given A_i and B_i, the linear slope of SS for (11) can be computed by

$$C_i = R^{-1}(z) B_i^\top P_i \tag{12}$$

where P_i is the solution of

$$P_i A_i + A_i^\top P_i - P_i B_i R^{-1}(z) B_i^\top P_i + Q(z) = -\dot{P}_i. \tag{13}$$

Then, there exists a region that satisfies $\dot{V}_i < 0$ in the domain Ω_i assuring $\mathrm{Re}[\lambda_{1,\ldots,n-m}(A_{cl_i}(z))] < 0$ where $A_{cl_i}(z)$ appears in

$$\dot{\tilde{z}} = A_{cl_i}(z)\tilde{z} = [A_{11}(z) - A_{12}(z)C_i]\tilde{z}$$

if the following condition is satisfied

$$\gamma_i = \frac{\|g_i(z)\|_2}{\|\tilde{z}\|_2} < \gamma_{max} = \frac{1}{2} \frac{\lambda_{\min}(W(z))}{\|P_i\|_2} \tag{14}$$

where $W(z) = Q(z) + P_i B_i R^{-1}(z) B_i^\top P_i$ and $g_i(z) = [A_{11}(z) - A_{12}(z)C_i - A_{cl_i}]\tilde{z}$.

Proof. See Theorem 4 together with its proof proposed by Copur et al. (2019).

Theorem 5 is implemented by the following algorithm.

Algorithm 1: Implementation of Theorem 5

Initialization: $\tilde{z}(0) = \tilde{z}_0 \in \Omega_0$, $\Omega(z) \geq 0$, $R(z) > 0$, $i = 0$ and $0 < \varepsilon < 1$

1 $A_i = A_{11}(z)|_{z=z_i}$ and $B_i = A_{12}(z)|_{z=z_i}$;
2 Obtain P_i by solving SDRE in (13);
3 Compute C_i from (12);
4 Compute u in (8);
5 Solve (2) and (3) numerically by applying u;
6 **if** *the condition (14) is not satisfied* **then**
7 | Go to Step 2 with $z = z_{i+1}$ where z is computed at Step 5.;
8 **else**
9 | Go to Step 4;
10 **end**

4. SDRE-BASED SMC FOR A 3-DOF HELICOPTER

Theorem 5 implemented by Algorithm 1 has been applied to the control of a 3-DOF helicopter produced by Quanser Inc. Since SDRE-based SMC requires a model of the controlled plant, the model of 3-DOF helicopter is briefly presented. Then, the design method of the new SDRE-based SMC based on the 3-DOF helicopter model for a tracking task is clearly outlined.

4.1 Helicopter Model

3-DOF helicopter, as shown in Fig. 1, is capable of rotating around three orthogonal axes, namely elevation, pitch, and travel axes represented by θ, ϕ, and ψ, respectively. The laboratory set-up is equipped with two DC motors,

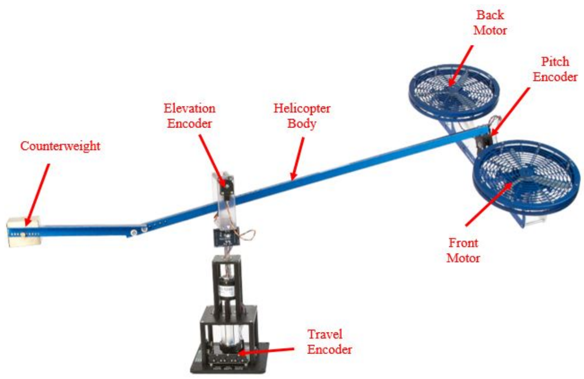

Fig. 1. 3-DOF Helicopter.

each attached to one end of the long arm to power one propeller. The embedded controller can manipulate V_b and V_f, denoting respectively the back and front motor voltages so that the cyclic thrust force τ_{cyc} and the collective thrust force τ_{coll} can be altered to control the helicopter's rotations. However, since the under-actuated nature of the helicopter only allows to control the rotations around two axes simultaneously, the other axis inherently becomes

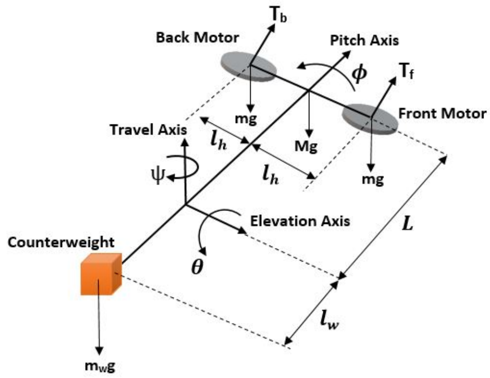

Fig. 2. Free-body diagram of 3-DOF Helicopter.

Table 1. Parameter Values of the Helicopter Model

Parameter	a_1	a_2	b_1	b_2	b_3	c_1	c_2
Value	0.2517	0.2105	0.3290	1.5664	16.200	7.3200	1.000
Parameter	d_1	d_2	d_3	e_1	e_2	α	
Value	0.1011	0.5040	1.3400	6.1600	1.000	4.000	

free to move. In addition, the rotational position around each axis is measured by using a high precise encoder for an feedback information accurate enough to compute an effective control input. In the light of the aforementioned information about the helicopter's dynamics and structure, its free-body diagram is given in Fig. 2. Given the state vector of the helicopter as

$$\left[\, x_1 \; x_2 \; \cdots \; x_8 \,\right]^\top = \left[\, \theta \; \phi \; \psi \; \dot{\theta} \; \dot{\phi} \; \dot{\psi} \; \tau_{cyc} \; \tau_{coll} \,\right]^\top, \tag{15}$$

its equations of motion has been previously derived by Ishutkina (2004) in the state-space form of

$$\begin{aligned}
\dot{x}_1 &= x_4 \\
\dot{x}_2 &= x_5 \\
\dot{x}_3 &= x_6 \\
\dot{x}_4 &= -d_1 x_4 - d_2 \sin(x_1) + d_3 x_8 \cos(x_2) \\
\dot{x}_5 &= -b_1 x_5 - b_2 \sin(x_2) - b_3 x_7 \\
\dot{x}_6 &= -a_1 x_6 - a_2 (\alpha x_8 + 1) \sin(x_2) \\
\dot{x}_7 &= -c_1 x_7 + 0.5 c_2 u_2 - 0.5 c_2 u_1 \\
\dot{x}_8 &= -e_1 x_8 + 0.5 e_2 u_1 + 0.5 e_2 u_2
\end{aligned} \tag{16}$$

where the control input vector u compounded of the motor voltages is given as $u = \left[\, u_1 \;\; u_2 \,\right]^\top = \left[\, V_f \;\; V_b \,\right]^\top$.

In addition, Ishutkina (2004) has also estimated the parameters of the nonlinear model in (16) that are given in Table 1. In this study, the same values have been utilized for designing SDRE-based SMC. Then, the extended linearization technique enables the state-space model in (16) to be factorized in the form of (1) through SDC matrices obtained by Kocagil et al. (2018). In addition, as mentioned in Section 2, to guarantee the solution of SDRE in (7), Lemma 1 must be satisfied. Fortunately, it can be computationally verified that $\{A(x), B(x)\}$ is pointwise stabilizable and controllable over a working state space.

4.2 SDRE-based SMC Design

In SDRE-based SMC, the error dynamics of 3-DOF model in (16) must be considered to achieve the desired performance in its rotational motions of interest. For this reason, the factorized model of 3-DOF helicopter is augmented by adding two more states, and this yield the following error dynamics, given by

$$\dot{e} = \hat{A}(e)\, e + \hat{B}(e)\, u \tag{17}$$

where the error vector $e = [x_e \; \tilde{x}_e]^\top$ including

$$x_e = [\theta_d - \theta \;\; \phi \;\; \psi_d - \psi \;\; \dot{\theta} \;\; \dot{\phi} \;\; \dot{\psi} \;\; \tau_{cyc} \;\; \tau_{coll}]^\top$$

and $\tilde{x}_e = \int [\theta_d - \theta \;\; \psi_d - \psi]^\top dt$. In addition, SDC matrices now become

$$\hat{A}(e) = \begin{bmatrix} A(x) & 0 \\ -\bar{A} & 0 \end{bmatrix} \text{ and } \hat{B}(e) = \begin{bmatrix} B(x) \\ 0 \end{bmatrix}$$

where the output matrix is selected to be

$$\bar{A} = \begin{bmatrix} 1 & 0 & 0 & 0 & 0 & 0 & 0 & 0 \\ 0 & 0 & 1 & 0 & 0 & 0 & 0 & 0 \end{bmatrix}$$

since the helicopter must follow the desired trajectories planned for both the elevation and travel axes. To design a sub-optimal SS, the error dynamics (17) is then converted into the structure of (2) and (3) by using $T^{-1}(e) = M(e)W(e)$ where, for $\hat{A}(e)$ computed at each instant of time, $M(e)$ is its controllability matrix and $W(e)$ includes the coefficients of its characteristic polynomial given by

$$W(e) = \begin{bmatrix} \hat{a}_9 & \hat{a}_8 & \cdots & \hat{a}_1 & 1 \\ \hat{a}_8 & \hat{a}_7 & \cdots & 1 & 0 \\ \vdots & \vdots & \vdots & \vdots & \vdots \\ \hat{a}_1 & 1 & \cdots & 0 & 0 \\ 1 & 0 & \cdots & 0 & 0 \end{bmatrix}.$$

Then, the matrix sub-blocks is obtained as $A(z) = T(e)\hat{A}(e)T^{-1}(e)$ and $B(z) = T(e)B(e) = [0 \;\; B_2(z)]^\top$.

Finally, the slope $C(z)$ in (4) can be optimally computed by using Algorithm 1 based on Theorem 5 which minimizes the modified cost function

$$J = \frac{1}{2}\int_0^\infty \left\{ \tilde{z}^\top(t) Q(\tilde{z})\, \tilde{z}(t) + \hat{z}^\top(t) R(\tilde{z})\, \hat{z}(t) \right\} dt \tag{18}$$

5. EXPERIMENTAL RESULTS

To evaluate the effectiveness of the proposed SDRE-based SMC developed in Section 3, it was bench-marked against the classical SDRE-based SMC presented in Section 2. With this aim, a set of experiments was conducted on the 3-DOF helicopter in Section 4. The real-time tracking control has been achieved by building the proposed SDRE-based SMC according to the design process in Subsection 4.2 with the nonlinear model in Subsection 4.1. In the experiments, the 3-DOF helicopter must follow the pre-defined trajectories in both travel and elevation axes without considering its motion in pitch axis due to the under-actuated mechanism.

Each experiment was started off from the initial angular positions selected to be $\theta(0) = -15°$ and $\phi(0) = \psi(0) = 0$ and lasted for 180s. In addition, a different staircase input was used for the reference trajectories in both axes. In the SDRE-based SMC design, the weighting matrix $Q(z)$ in (18) was chosen to be state-dependent such that

$$Q = \text{diag}(10 + \tilde{z}_1^2, \text{abs}(\tilde{z}_2), 10 + \tilde{z}_3^2, .1, .1, .1, 1 + \tilde{z}_7^2, 1 + \tilde{z}_8^2)$$

with a 2×2 identity matrix R to solve the augmented SDRE (18). In addition, k in the nonlinear control law

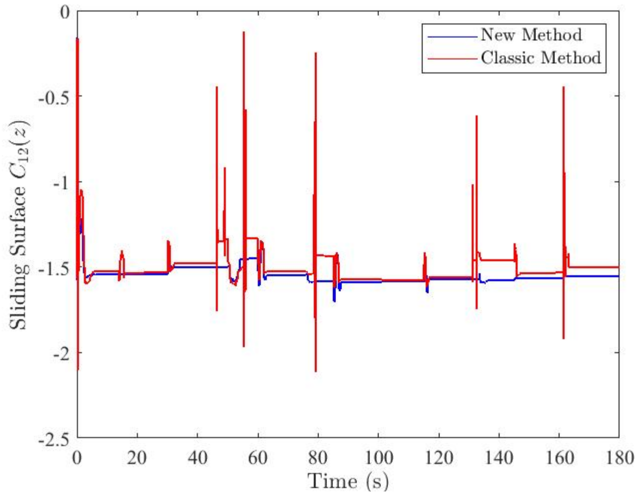

Fig. 3. Slopes of sliding surface $C_{12}(z)$ designed by classic and new SDRE-based SMC

(10) was selected to be 3 and the sampling frequency was selected to be 200 Hz.

Due to the dimensions of the state and control input vectors of the 3-DOF helicopter model, SS becomes a 2×8 matrix. Therefore, only one SS slope is arbitrarily selected and here depicted because of the limited space. Fig. 3 shows the changes in the selected SS slope ($C_{12}(z)$) computed by (6) of the classical SDRE-based SMC and (12) of the new SDRE-based SMC. It is obvious that the implementation of the classical SDRE-based SMC results in sharper changes in SS slope, especially when the desired trajectory is reshaped. However, the new SDRE-based SMC can facilitate smoother transition at these instants of time. In addition, the new SDRE-based SMC does not require the re-computation of SS slope as lonat each instant of time, hence the need of less computational load. This appears itself as a straight line in Fig. 3. It is also important to investigate the effects of the new SDRE-based SMC on the desired control performance.

Fig. 4 and Fig. 5 show the time responses of the 3-DOF helicopter in its elevation and travel axes, respectively. From the experimental results, it is apparent that the new SDRE-based SMC provides the same control performance as the classic. It is even able to produce better transient response characteristics. For example, less maximum overshoots at both 60s and 140s are observed in the transient response of the helicopter. In addition, since dramatic changes in SS slopes are eliminated, the new SDRE-based SMC also decreases the required control input levels for the tracking control.

In Fig 6 and Fig 7, the front and back motor voltages are given, respectively. As can be seen here, rather than the classic SDRE-based SMC, the proposed enables the helicopter to track the desired trajectories in both axes by generating less control inputs. In addition, the spikes at the instants of time, when the step reference is changed, can be also eliminated in the new method.

6. CONCLUSION

This study was aimed to incorporate SMC with a new SDRE method for designing a sub-optimal SS, which does

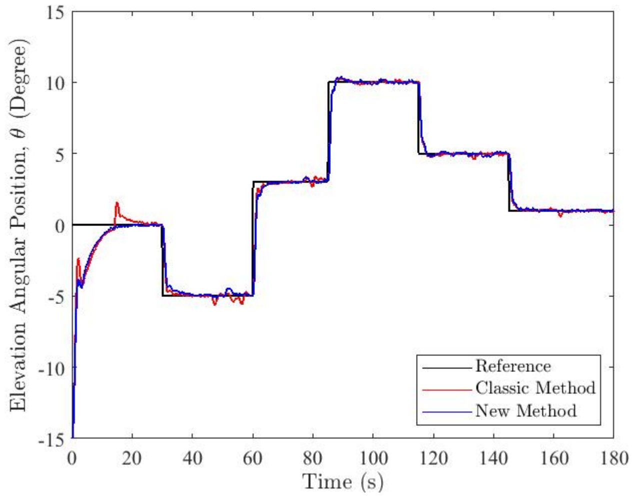

Fig. 4. Elevation responses of the helicopter controlled by classic and new SDRE based methods

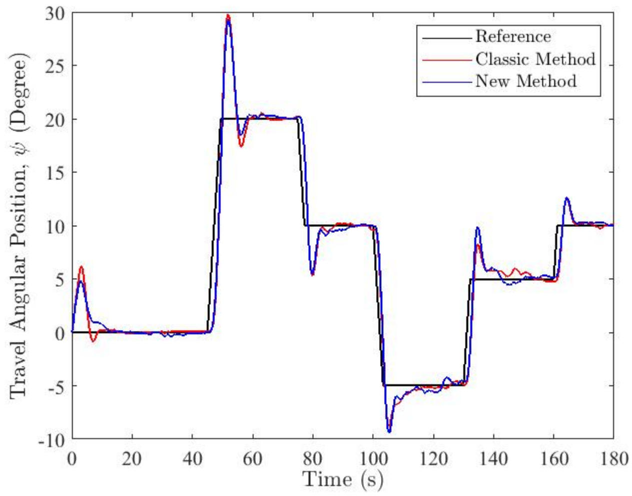

Fig. 5. Travel responses of the helicopter controlled by classic and new SDRE based methods

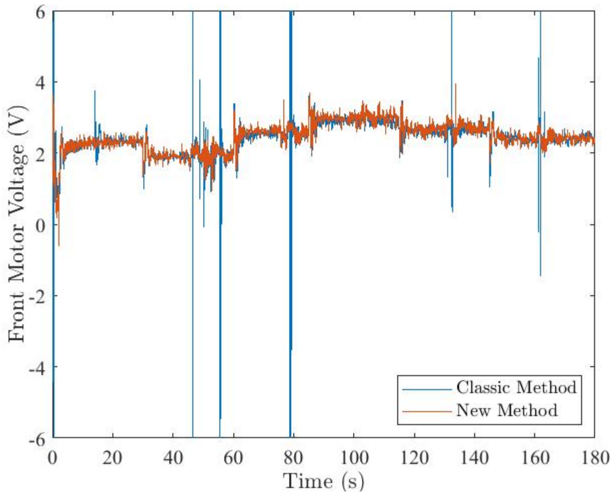

Fig. 6. Control inputs to the front motor of the helicopter controlled by the classical and new methods

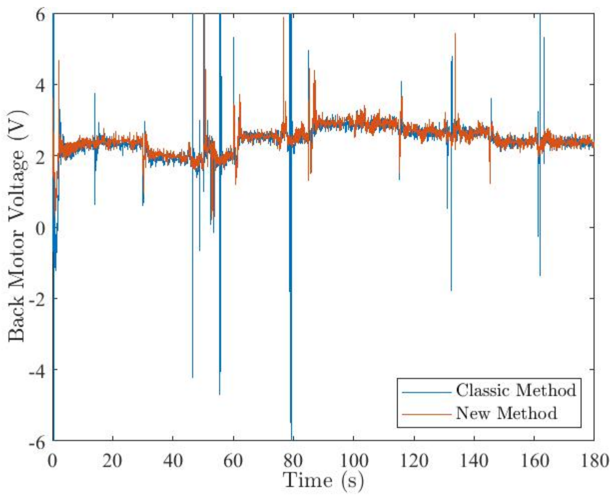

Fig. 7. Control inputs to the back motor of the helicopter controlled by the classical and new methods

not suffer from the issues of the classical SDRE method, i.e. possible instability and computational burden. The effectiveness of the proposed control method was experimentally investigated on a 3-DOF helicopter laboratory. In the experiments, both the classical and new SDRE-based SMC were designed for a tracking control problem. The comparative results reveal that the new SMC can produce smoother SS slope as well as less computational load and control inputs without degrading the control performance.

REFERENCES

Adhikary, N. and Mahanta, C. (2018). Sliding mode control of position commanded robot manipulators. *Control Engineering Practice*, 81, 183–198.

Bilgin, N. and Salamci, M.U. (2014). Sliding mode control design for nonlinear systems without reaching phase and its applications to a flexible spacecraft. In *ASME 2014 12th Biennial Conference on Engineering Systems Design and Analysis*, 1 – 9. ASME, Copenhagen, Denmark.

Çimen, T. (2010). Systematic and effective design of nonlinear feedback controllers via the state-dependent riccati equation (SDRE) method. *Annual Reviews in Control*, 34(1), 32–51.

Çimen, T. (2012). Survey of state-dependent riccati equation in nonlinear optimal feedback control synthesis. *Journal of Guidance, Control, and Dynamics*, 35(4), 1025–1047.

Copur, E.H., Arican, A.C., Ozcan, S., and Salamci, M.U. (2019). An update algorithm design using moving region of attraction for SDRE based control law. *Journal of the Franklin Institute*, 356(15), 8388–8413.

Corradini, M.L. and Cristofaro, A. (2018). Nonsingular terminal sliding-mode control of nonlinear planar systems with global fixed-time stability guarantees. *Automatica*, 95, 561–565.

Edwards, C., Alwi, H., and Hamayun, M.T. (2018). Fault tolerant control using integral sliding modes. In S. Li, X. Yu, L. Fridman, Z. Man, and X. Wang (eds.), *Advances in Variable Structure Systems and Sliding Mode Control—Theory and Applications*, volume 115 of *Studies in Systems, Decision and Control*, chapter 13, 305–338. Springer International Publishing, Cham, Switzerland.

Farrage, A. and Uchiyama, N. (2018). Energy saving in biaxial feed drive systems using adaptive sliding mode contouring control with a nonlinear sliding surface. *Mechatronics*, 54, 26–35.

Ishutkina, M.A. (2004). *Design and Implementation of a Supervisory Safety Controller for a 3DOF Helicopter*. mathesis, Massachusetts Institute of Technology, USA.

Kocagil, B.M., Ozcan, S., Arican, A.C., Guzey, U.M., Copur, E.H., and Salamci, M.U. (2018). Adaptive control of a 3 DoF helicopter with linear and nonlinear reference models. In *2018 6th International Conference on Control Engineering and Information Technology (CEIT)*.

Lee, H. and Utkin, V.I. (2007). Chattering suppression methods in sliding mode control systems. *Annual Reviews in Control*, 31(2), 179–188.

Liang, W., Yongzhi, S., and Xiangdong, L. (2013). SDRE based adaptive optimal sliding mode control for re-entry vehicle. In *Proceedings of the 32nd Chinese Control Conference*, 435 – 440. Xi'an, China.

Mobayen, S. and Baleanu, D. (2015). Stability analysis and controller design for the performance improvement of disturbed nonlinear systems using adaptive global sliding mode control approach. *Nonlinear Dynamics*, 83(3), 1557–1565.

Mobayen, S., Tchier, F., and Ragoub, L. (2017). Design of an adaptive tracker for n-link rigid robotic manipulators based on super-twisting global nonlinear sliding mode control. *International Journal of Systems Science*, 48(9), 1990–2002.

Ozcan, S., Salamci, M.U., and Nalbantoglu, V. (2020). Multiloop state-dependent nonlinear time-varying sliding mode control of unmanned small-scale helicopter. *Proceedings of the Institution of Mechanical Engineers, Part G: Journal of Aerospace Engineering*, 234(3), 585–606.

Pieper, J. and Surgenor, B. (1993). Discrete sliding control of a coupled-drives apparatus with optimal sliding surface and switching gain. *IEE Proceedings D Control Theory and Applications*, 140(2), 70.

Salamci, M.U. and Gökbilen, B. (2007). SDRE missile autopilot design using sliding mode control with moving sliding surfaces. *IFAC Proceedings Volumes*, 40(7), 768–773.

Tai, T.L. and Lu, Y.S. (2006). Global sliding mode control with chatter alleviation for robust eigenvalue assignment. *Proceedings of the Institution of Mechanical Engineers, Part I: Journal of Systems and Control Engineering*, 220(7), 573–584.

Utkin, V. (1977). Variable structure systems with sliding modes. *IEEE Transactions on Automatic Control*, 22(2), 212–222.

Utkin, V.I. (1992). *Sliding Modes in Control and Optimization*, chapter 7, 101. Springer Berlin Heidelberg.

Yan, X.G., Spurgeon, S.K., and Edwards, C. (2017). *Variable Structure Control of Complex Systems*, chapter 1, 4–12. Springer International Publishing, Cham, Switzerland.

Yu, X. and Kaynak, O. (2016). Soft computing methodologies in sliding mode control. In B.M. Wilamowski and J.D. Irwin (eds.), *The Industrial Electronics Handbook Control and Mechatronics*, chapter 22, 22.1–22.12. CRC Press, Boca Raton, 2 edition.